

Experimental research of condensation processes occurring under laser ablation in superfluid helium and vacuum

E. B. Gordon, M. I. Kulish¹, M. E. Stepanov¹, V. I. Matyushenko²,
and A. V. Karabulin^{1,3,4}

¹*Institute of Problems in Chemical Physics of RAS
Chernogolovka 142432, Moscow Region, Russia*

²*Chernogolovka Branch of the N. N. Semenov Federal Research Center for Chemical Physics of RAS
Chernogolovka 142432, Moscow Region, Russia*

³*Joint Institute for High Temperatures of RAS, Moscow 125412, Russia*

⁴*National Research Nuclear University MEPhI (Moscow Engineering Physics Institute)
Moscow 115409, Russia*

E-mail: avkarabulin@gmail.com

Received February 2, 2020, published online July 22, 2020

The dynamics of thermal radiation accompanying the condensation of tungsten nanoparticles in superfluid helium and vacuum was studied experimentally in the visible range. It was shown that during the first 100 μ s the accompanying thermal energy of process in the case of superfluid helium is considerably higher than in vacuum at comparable temperatures after that it levels up. From a standpoint of the process' kinetics it is demonstrated that the reasons for this are, on one hand, an increased condensation rate in superfluid helium (due to the concentration of nanoparticles in quantized vortices), and on the other hand, higher efficiency of heating of the condensation products in superfluid helium (due to the prevalence of processes involving particles of similar sizes).

Keywords: condensation of tungsten nanoparticles, thermal emission, superfluid helium.

1. Introduction

The processes of low-temperature condensation of sub-micron and nanoparticles represent a very interesting object for research, both from fundamental and applied points of view. In particular, they are important for studies of the evolution of interstellar dust occurring in space, including the processes of its destruction and recovery [1–5]. The main source of information about these processes is the studies of the accompanying radiation [6]. However, in recent years successful attempts have been made in laboratory simulations of the conditions close to those actually existing in interstellar dust clouds (low temperatures and densities) [7]. As the examples of such methods developed recently one can consider the study of coagulation processes in neon matrices [8], in cold helium droplets [9, 10] and the condensation on cold surfaces [11].

Our low-temperature experiments on the condensation of particles in the volume of superfluid helium (He II) also provide conditions that simulate those encountered in space.

Indeed, as we established earlier, long thin nanowires are formed [12, 13] upon the condensation of products of laser ablation of metals in the bulk of superfluid helium. Both, their diameters and structure are well described in the framework of the scenario proposed in [14]. The latter includes the concentration of metal nanoparticles in quantized vortices and their melting during mutual fusion due to the heat released at the expense of a decreasing surface energy. The existence of strong local overheating was justified by the possibility of destruction of superfluidity around the condensation product with subsequent evaporation of helium and formation of a shell filled with a rarefied gas, which insulates the heat removal [15].

Pyrometric experiments on measuring a temporal behavior of the thermal radiation accompanying the condensation of various metals in He II have shown that the temperature of the condensation products correlates with the melting temperature of the metal, significantly exceeding it only during the early stages of the condensation process [16]. Therefore, it was concluded that each individual condensation act proceeds practically adiabatically.

Nevertheless, even assuming the process of metal condensation in He II to be completely adiabatic, it may yet differ from the one in vacuum. Naturally, the characteristics of the elementary act of fusion itself, of subsequent melting, and a change in the shape of the product particle in a vacuum and a bubble filled with rarefied helium cannot diverge noticeably. However, there may be several fundamental and important differences.

First of all, in superfluid helium there is a fast fusion of particles trapped in the vortices [17–19] along with the diffusion-controlled process in the bulk. This is not the case in vacuum, gas and ordinary liquid. Due to the one-dimensionality of the vortex, trapped particles move strictly towards each other, and therefore the probability of their collision is much higher than in a volume where the directions of particle velocities are distributed randomly. Since at low temperatures any collision of metal particles leads to their condensation, the rate of the latter in He II is much higher than in the volume of gas and can be higher than in vacuum.

Secondly, the larger the condensation product in He II becomes, the longer it lives in the core of the vortex [20, 21]. Thus, in superfluid helium the process of collision of particles gains its specifics: the probability of collision of large and similar-sized particles begins to prevail almost immediately. In other words, “coagulation” becomes predominant there, whereas in any medium where the probability of collisions does not depend on particle volume, mainly different-sized particles will collide, resulting in collecting of small particles on a large centers, i.e. “accretion” will be occurring.

Based on the foregoing logic, it can be assumed that in vacuum the accretion will be taking place, and hence the change in surface energy and, consequently, the heating will be small. Therefore, during the condensation of particles in the He II volume, both the intensity of thermal emission and color temperature can be assumed to be noticeably higher than that in vacuum. The aim of the investigation was to test these differences experimentally.

2. Experimental

Experimental technique and apparatus employed here were described in detail in [16]. The simplified view of the experimental setup is shown in Fig. 1. Its basis was a pumped-out helium cryostat equipped with optical windows ($d_w = 40$ mm). Through the front window the ablation of the target located inside the cryostat was carried out by using a solid-state Nd:LSB laser with the following characteristics: wavelength $\lambda = 1.062$ μm , pulse energy $E = 0.1$ mJ, pulse duration $\tau = 0.4$ ns and pulse repetition rate $f = 50$ Hz. Through the side window, the thermal radiation from condensing ablation products fell into a photomultiplier (PMT) with a gate function. Details of the used pyrometric technique can also be found in [16]. With its help, the dependences of thermal radiation on time were

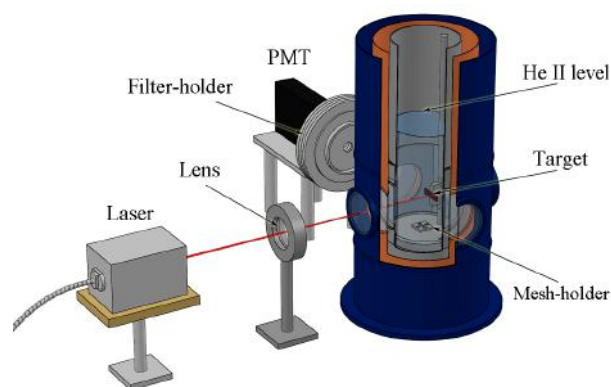


Fig. 1. Simplified scheme of experimental setup.

measured, which enable to calculate color temperatures of the ongoing.

As in [16], the emission spectrum was determined using a set of narrow-band (~ 10 nm) interference filters (Thorlabs) from 400 to 700 nm with a step of 50 nm and a reference source (incandescent lamp SLS201L (Thorlabs)) with a given brightness temperature of 2796 K, which made it possible to carry out quantitative estimates of the temperature of the studied processes. Tungsten was chosen as an object of the study because of its high melting point in order to maximize the intensity of thermal emission during condensation.

The temperature was maintained constant by pumping out helium vapor and amounted to $T \approx 1.2$ K (which corresponds to a vapor pressure of less than 1 Torr) during working in superfluid helium. Ablation in vacuum was carried out at room temperature and pressure of 10^{-3} Torr. The geometry of the entire system remained unchanged during ablation in both media: superfluid helium and vacuum.

In both cases, the condensation products settled to the bottom of the experimental cell, where copper or gold grids 3 mm in diameter, coated with a perforated carbon film, commonly used in transmission electron microscopy (TEM) were placed in special holder. After warming the cryostat to room temperature, the samples were studied in a JEOL JEM-2100 electron microscope.

3. Results and discussion

Micrographs of the condensation products of tungsten in superfluid helium upon irradiation of its surface with a laser pulse in vacuum and He II are shown in Fig. 2. Spherical clusters with diameters of up to about 250 nm are formed in vacuum, whereas in He II the result of condensation is represented by metal structures incorporated in a network in which individual wires are interconnected at points of contact and have diameters of about 2 nm.

The obtained time dependences $T(t)$ of temperature is shown in Fig. 3. It can be seen that apart from the initial stage when T is significantly higher, the color temperature of the processes is close to the melting point of tungsten ($T_m = 3695$ K), being slowly decreasing with time. It can also be noticed that cooling in vacuum is slower than in

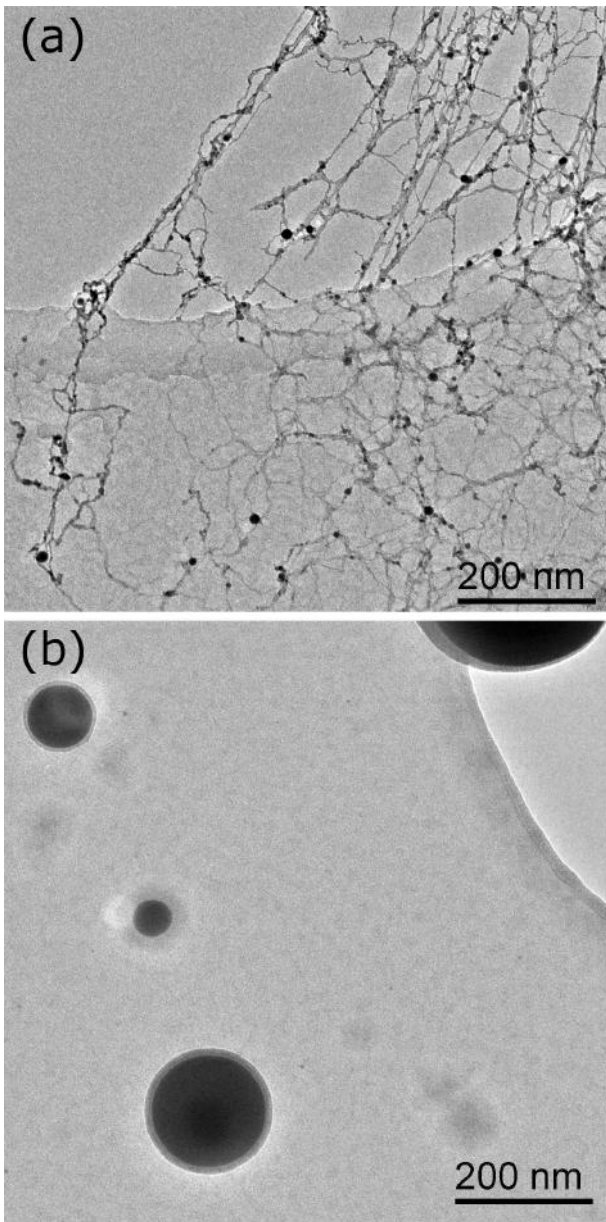


Fig. 2. TEM of condensation products, grown during of ablation of tungsten target in superfluid helium (a) and in vacuum (b) and collected on TEM meshes.

He II, which can be explained if taking into account that irradiation is the only possible energy-release channel in vacuum.

Of greatest interest are the data in Fig. 4(a), which shows the time dependences of the glow intensity $I(t)$ at 700 nm (the wavelength $\lambda = 700$ nm is close to the maximum spectral intensity for the blackbody at observed temperatures). One can see that the radiation intensity of nanoparticles strongly depends on time and decreases by about three orders of magnitude during the observation time of ~ 200 μ s. During ablation in superfluid helium, the condensation takes place within several millimeters from the target surface [16, 22]. In vacuum, the expansion velocity for

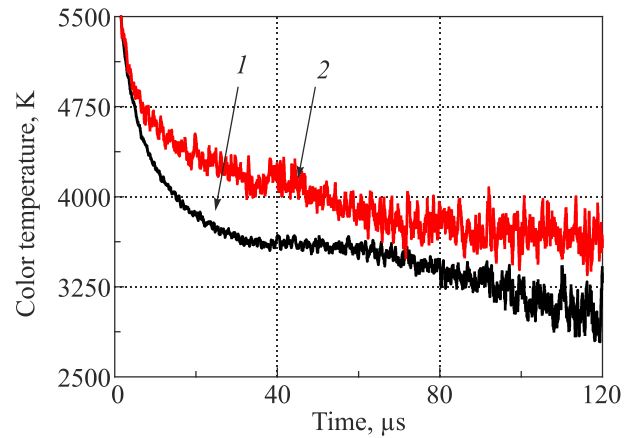


Fig. 3. The color temperature of thermal emission accompanying the condensation of tungsten clusters in He II (1), vacuum (2) obtained from the radiation spectra.

nanoparticle formed upon laser ablation (as in our case) is around 100 m/s [23], so that, in $t = 200$ μ s, the nanoparticles cover distance $L = 20$ mm and remain within the field of view. It means that, in both cases, the radiation is collected from the entire volume in which condensation occurs. Therefore, we can assume that the obtained dependences reflect the kinetics of the total energy that is being released during condensation.

The most significant result appears to be the fact that the thermal radiation $I(t)$ in He II substantially exceeds that in vacuum for a considerable time, despite the fact that the temperature in vacuum is higher, and therefore the radiation power is higher there likewise. If we remain within the framework of the reasonable assumption that the collision-resulted fusion itself proceeds identically for identical particles in both media, then the increase in the signal $I(t)$ can be explained by two reasons:

(1) Reaction rates may vary, since the observed irradiation $I(t)$ is proportional to the frequency of condensation events as causing the local heating. In other denotation, $I \sim -dn/dt$, where the derivative on the right side is the rate of decrease in the concentration n of ablation products with time.

(2) Not every condensation act contributes to the measured signal I due to the limited sensitivity range of the PMT. To describe this effect, it is convenient to introduce a proportionality coefficient ϵ , which has the meaning of the probability of light emission in the visible (recorded) range during particle collisions. The fact is that due to the high temperature of tungsten nanoclusters and the large ratio of their surface to volume, the time of radiation cooling of the nanowires to temperatures lower than those recorded by our method (less than 1500 K) is short compared to other characteristic times. Therefore, radiation has the nature of individual light pulses, the energy of which and, consequently, the quantity ϵ , depends only on the mass ratio of the colliding particles. The case of coagulation is

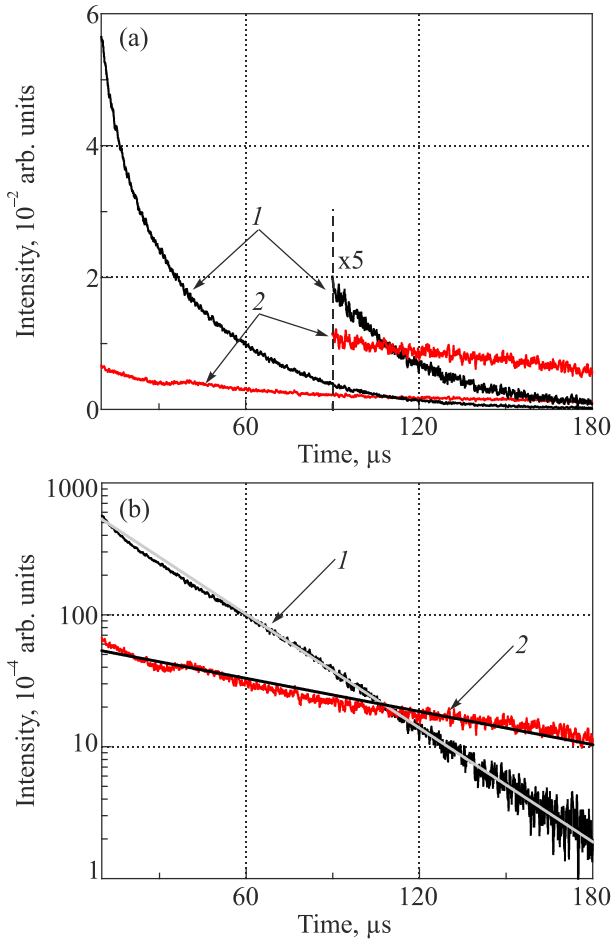


Fig. 4. (a) time dependences of the radiation intensity accompanying the condensation of tungsten in He II (1), and in vacuum (2). (b) anamorphoses in semilogarithmic coordinates (decimal logarithm) of the experimental dependences of the intensity of thermal radiation on time for the condensation of the products of tungsten ablation occurring in He II (1), and vacuum (2). The dashed line shows linear approximations by which the relationships between the rates of coagulation reactions and their initial intensities were determined.

the most favorable for our registration method: when nanoparticles of a similar size collide the temperature raises significantly due to a major change in the surface energy, so the probability of emission $\varepsilon \rightarrow 1$, and the corresponding thermal radiation, in accordance with Wien's law, falls in registered visible range. In the opposite case of accretion, the temperature barely increases due to the small redistribution of surface energy, $\varepsilon \rightarrow 0$. Thereby the act of accretion does not lead to irradiance in the observed range.

Initially, both reasons for the increase in the signal in He II relative to vacuum take place since on the one hand, the reaction of condensation is accelerated by vortices, which leads to an increased consumption of ablation products $-dn/dt$, and on the other hand, the coagulation process can be expected to prevail in He II over accretion, which means an increase of the probability of emission ε .

Thus $I \sim -\varepsilon * dn/dt$, and it was necessary to find out which of the two effects was more likely the reason of an increase in the radiation intensity in He II.

As can be seen from Fig. 4(b), both in He II and in vacuum at times exceeding 30 μs the dependence of the intensity on time is well approximated by the exponent, which is evidence of first-order kinetics, i.e., the following relations take place:

$$\frac{dn(t)}{dt} = -kn(t), \quad (1)$$

$$n(t) = n_0 \exp(-kt). \quad (2)$$

With their help, it is possible to estimate the values of the signal $I(t)$ recorded by PMT:

$$I(t) \sim -\varepsilon \frac{dn(t)}{dt} = \varepsilon kn(t) = \varepsilon kn_0 \exp(-kt) \sim I^0 \exp(-kt), \quad (3)$$

where $I^0 \sim \varepsilon kn_0$ is the amplitude of the signal at the first moment of registration, proportional to three quantities: ε — the probability of the emission of thermal energy in visible light; initial concentration n_0 of ablation products; and rate constant k [sec^{-1}], which, on the one hand, has the meaning of the probability of condensation, and on the other hand, $k = 1/\tau$, where the characteristic time τ is the time of e-folded decreasing of the signal.

More conclusions can be drawn if considering a behavior of the initial irradiance amplitudes I^0 in more detail. As our experiments show, in vacuum and superfluid helium the ablation efficiency is almost the same.

Can one then assume that the magnitude of the probability of emission ε is also the same in both media? If that was the case, then, as can be seen from (3), the initial amplitudes $I^0 \sim \varepsilon kn_0$ should be in the same proportion as the rate constants k . From the slope of the curves in Fig. 4(b) rate constants k , defined as the slopes of the logarithmic anamorphoses of kinetic curves, are related to as $k_{\text{He II}}:k_{\text{vac}} = 3.5:1$. Therefore, the same relation should be fulfilled for the initial amplitudes. However, it follows from Fig. 4(a) that $I_{\text{He II}}^0:I_{\text{vac}}^0 = 10:1 \neq k_{\text{He II}}:k_{\text{vac}}$.

This means that the assumption that ε is independent of the medium is false, which can be explained by the fact that in He II the probability of emission ε for one condensation event is almost three times higher than in vacuum, which, as it was discussed above, is in a good agreement with influence on the condensation process of quantized vortices.

It is also important to emphasize that at a time of 100 μs the intensities in superfluid helium and gas equalize, which can be seen from the intersection of the curves (highlighted separately in Fig. 4). This suggests a gradual slowdown in the process of heat release in helium and the transition of the ensemble of particles to the stage of pure cooling, which is no longer supported by additional sources of heat, and moreover, which is cooling rapidly. An increase in the

cooling rate in helium relative to vacuum at longer times is directly indicated by the growing difference in temperatures for the two media (see Fig. 3). Apparently, this is due to the gradual depletion of nanomaterial for the formation of networks of nanowires, which reduces the number of collisions leading to heat release.

Furthermore, in light of this reduction, at certain moments, which may differ for each individual hot spot, a strong cooling channel of helium heat transfer may be appearing, in addition to irradiative cooling. This results in the intensity curve corresponding to He II to pass below the one corresponding to vacuum.

Indeed, if there was no additional cooling channel in helium, then, given the higher temperature of the clusters in vacuum, the curves should not intersect since the more the body is heated, the higher is the power of thermal radiation. If that was the case, we would have to see faster irradiative cooling for hotter particles, that is, for particles in a vacuum. However, the curves still intersect, which can only be explained by more efficient cooling in helium.

4. Conclusions

The processes of condensation of products of pulsed laser ablation were experimentally studied in two media: in vacuum and superfluid helium. In both cases, the intensity of thermal radiation accompanying the condensation of tungsten nanoparticles decreases exponentially with time, however, there is a significant difference in its initial values and the dynamics of decline. For the equal ablation efficiency and comparable temperatures, the initial radiation intensity in superfluid helium significantly (more than an order of magnitude) exceeds that in vacuum, while its decline rate is also significantly higher. Analyzing the kinetics of thermal radiation, it is shown that this difference can be explained by the catalysis of the coalescence of atoms and small metal clusters by quantized vortices in He II. In this case, quantized vortices have a double role: 1) increase the rate of condensation due to the concentration of the initial particles in the vortex; 2) increase the efficiency of heating the condensation products in He II due to the prevalence of processes involving particles of close size. Ultimately, the condensation of products of laser ablation of a tungsten target in a vacuum results in spheres with a diameter of 50–250 nm, and in He II in webs, consisting of nanowires with a diameter of 2 nm.

The work was financially supported by RSF (project № 18-19-00620).

1. B. T. Draine, *ArXiv:0903.1658* [Astro-Ph] (2009).
2. B. Stepanik, A. Abergel, J.-P. Bernard, F. Boulanger, L. Cambrésy, M. Giard, A. P. Jones, G. Lagache, J.-M. Lamarre, C. Meny, F. Pajot, F. Le Peintre, I. Ristorcelli, G. Serra, and J.-P. Torre, *A&A* **398**, 551 (2003).
3. S. Zhukovska, H.-P. Gail, and M. Trieloff, *A&A* **479**, 453 (2008).

4. S. Zhukovska, T. Henning, and C. Dobbs, *Astrophys. J.* **857**, 94 (2018).
5. J. C. Weingartner and B. T. Draine, *Astrophys. J.* **517**, 292 (1999).
6. T. Henning, *Annu. Rev. Astron. Astrophys.* **48**, 21 (2010).
7. L. Colangeli, Th. Henning, J. R. Brucato, D. Clement, D. Fabian, O. Guillois, F. Huisken, C. Jäger, E. K. Jessberger, A. Jones, G. Ledoux, G. Manico, V. Mennella, F. J. Molster, H. Mutschke, V. Pirronello, C. Reynaud, J. Roser, G. Vidali, and L. B. F. M. Waters, *A&A Rev.* **11**, 97 (2003).
8. G. Rouillé, C. Jäger, S. A. Krasnokutski, M. Krebsz, and T. Henning, *Faraday Discuss.* **168**, 449 (2014).
9. S. A. Krasnokutski, G. Rouillé, C. Jäger, F. Huisken, S. Zhukovska, and Th. Henning, *Astrophys. J.* **782**, 15 (2014).
10. S. A. Krasnokutski, M. Goulart, E. B. Gordon, A. Ritsch, C. Jäger, M. Rastogi, W. Salvenmoser, Th. Henning, and P. Scheier, *Astrophys. J.* **847**, 89 (2017).
11. D. Fulvio, S. Göbi, C. Jäger, Á. Kereszturi, and T. Henning, *Astrophys. J. Suppl. Ser.* **233**, 14 (2017).
12. P. Moroshkin, V. Lebedev, B. Grobety, C. Neururer, E. B. Gordon, and A. Weis, *Europhys. Lett.* **90**, 34002 (2010).
13. E. B. Gordon, A. V. Karabulin, V. I. Matyushenko, V. D. Sizov, and I. I. Khodos, *Fiz. Nizk. Temp.* **36**, 740 (2010) [*Low Temp. Phys.* **36**, 590 (2010)].
14. E. B. Gordon, A. V. Karabulin, V. I. Matyushenko, V. D. Sizov, and I. I. Khodos, *J. Exp. Theor. Phys.* **112**, 1061 (2011).
15. J. Fang, A. E. Dementyev, J. Tempere, and I. F. Silvera, *Rev. Sci. Instrum.* **80**, 043901 (2009).
16. E. B. Gordon, M. I. Kulish, A. V. Karabulin, V. I. Matyushenko, and M. E. Stepanov, *J. Quant. Spectr. Radiat. Transf.* **222–223**, 180 (2019).
17. R. J. Donnelly, *Quantized Vortices in Helium II*, Cambridge University Press, Cambridge, England, New York (1991).
18. E. B. Gordon, *Fiz. Nizk. Temp.* **38**, 1320 (2012) [*Low Temp. Phys.* **38**, 1043 (2012)].
19. U. Giuriato and G. Krstulovic, *Sci. Rep.* **9**, 4839 (2019).
20. E. B. Gordon and Y. Okuda, *Fiz. Nizk. Temp.* **35**, 278 (2009) [*Low Temp. Phys.* **35**, 209 (2009)].
21. D. Mateo, J. Eloranta, and G. A. Williams, *J. Chem. Phys.* **142**, 064510 (2015).
22. E. B. Gordon, M. I. Kulish, A. V. Karabulin, and V. I. Matyushenko, *Fiz. Nizk. Temp.* **43**, 1354 (2017) [*Low Temp. Phys.* **43**, 1086 (2017)].
23. S. Amoroso, R. Bruzzese, X. Wang, N. N. Nedialkov, and P. A. Atanasov, *J. Phys. D* **40**, 331 (2007).

Експериментальне дослідження процесів конденсації, які відбуваються при лазерній абляції у надплинному гелії та вакуумі

Є. Б. Гордон, М. І. Куліш, М. Є. Степанов,
В. І. Матюшенко, А. В. Карабулін

Динаміку теплового випромінювання, що супроводжує конденсацію наночастинок вольфраму у надплинному гелії та вакуумі, експериментально досліджено у видимому діапазоні.

Показано, що протягом перших 100 мкс тепла енергія, яка супроводжує процес у надплинному гелії, набагато перевищує відповідну енергію у вакуумі при порівнянних температурах, після чого вона вирівнюється. Причинами цього є, по-перше, збільшення швидкості конденсації у надплинному гелії (через концентрацію наночастинок у квантованих вихорах) та,

по-друге, більш висока ефективність нагрівання продуктів конденсації у надплинному гелії (через перевагу процесів із залученням частинок близьких розмірів).

Ключові слова: конденсація наночастинок вольфраму, тепла емісія, надплинний гелій.